Excitation and decay of the Gamow-Teller giant resonance in ^{90}Nb

M. Moosburger,* E. Aschenauer,† H. Dennert, W. Eyrich, A. Lehmann,‡ N. Scholz,§ and H. Wirth**
Physikalisches Institut, Universität Erlangen, D-91058 Erlangen, Germany

H. J. Gils, H. Rebel, and S. Zagromski
Forschungszentrum Karlsruhe, Institut für Kernphysik III, D-76021 Karlsruhe, Germany
(Received 17 April 1997)

The proton decay of spin-isospin strength in ^{90}Nb was investigated after excitation via the reaction ^{90}Zr(^{6}Li,^{6}He)^{90}Nb at 156 MeV bombarding energy. The Gamow-Teller (GT) strength distribution and corresponding B(GT) values were extracted from singles spectra measured at extreme forward angles including zero degree. Protons in coincidence with ^{6}He ejectiles were detected using a multidetector arrangement of semiconductor strip detectors. Relative branching ratios and ^{6}He-p angular correlations have been measured for a proton decay to well defined low lying single hole states in ^{89}Zr. Evidence for a dominant statistical decay has been found in the whole observed region of excitation energy; a small direct decay component, however, cannot be ruled out. In the region of the Gamow-Teller giant resonance between 8.0 and 12.0 MeV excitation energy additional strength with higher mulitpolarities $L \geqslant 1$ was identified from a comparison with predictions in the statistical decay model. At higher excitation energies above the giant resonance region the decay characteristics confirm the presence of a flat distribution of Gamow-Teller strength. [S0556-2813(98)03302-0]

PACS number(s): 24.30.Cz, 25.70.Kk, 27.60.+j

I. INTRODUCTION

The study of collective excitations by charge exchange reactions has provided direct information on spin-isospin dependent phenomena in nuclear excitations [1]. Since their early theoretical prediction and systematical investigations using mainly the (p,n) reaction at intermediate energies, the Gamow-Teller (GT) resonances have gained special interest. The approximate proportionality of zero degree cross sections and B(GT) values can be explained by the role of the GT-transition operator describing both, the β-decay in nuclei and the reaction mechanism of the charge exchange reaction at small momentum transfer. Surprising, however, and still not completely resolved is the fact that the observed Gamow-Teller transition strength is only about two thirds of the prediction of a model independent sum rule [2]. This so called ''problem of missing GT strength'' was explained by the influence of subnuclear degrees of freedom shifting strength into the region of Δ excitation or/and by nuclear configuration mixing leading to broad and structureless strength distributions hidden in the physical continuum [3–8].

In this context it seems of special interest to investigate the decay properties of the GT giant resonance [9]. As long as the collective resonance can be described microscopically as a coherent sum of one-proton particle one-neutron hole states the measurement of the proton decay to various open channels can give valuable information on the microscopic structure of the giant resonance. If the decay proceeds through coupling to more-particle more-hole configurations the relative population of the different final states follows statistical rules and can give informations on the spins and multipolarities of the decaying strength. Thus the study of the relative contribution of the escape width representing the direct decay branch to neutron hole states and of the spreading width which reflects the statistical decay through configuration mixing is decisive for the understanding of the structure and the distribution of the Gamow-Teller strength.

Experimentally the decay properties of the giant resonances can be investigated by the coincident measurement of decay particles after excitation by a charge exchange reaction. But in contrast to isoscalar electric giant resonances, where the decay via emission of neutrons or charged particles is investigated over a wide range of target nuclei [9,10], only a few attempts have been made to measure the decay properties of the GT giant resonance. As mentioned before, GT resonances were mostly investigated by use of the (p,n) reaction at bombarding energies of about 200 MeV, where the ratio of $V_{\sigma\tau}/V_{\sigma}$ of the effective nucleon-nucleon interaction favors a spin transfer reaction ($\Delta S = 1$). At a reaction angle of $\Theta_n = 0°$ the Gamow-Teller cross section with multipolarity $L = 0$ is in a maximum. But decay measurements are very difficult there, suffering from the low efficiency and energy resolution of the time of flight technique for measuring high energy neutrons. An early attempt using the (^{3}He,t) reaction [11] has more recently been supplemented [13] by measurements over a range of target nuclei at a bombarding energy of 450 MeV and $\Theta = 0°$. Similar to the (p,n) reaction, at higher energies preferably spin-isospin modes are excited, although strength with $\Delta S = 0$ can contribute. Especially transitions to the isobaric analog state (IAS) appear in the excitation spectra and were

*Present Address: Sektion Physik, Ludwig-Maximilians-Universität München, D-85748 Garching, Germany.
†Present Address: DESY, D-22603 Hamburg, Germany.
‡Present Address: Paul Scherrer Institut, CH-5232 Villigen, Switzerland.
§Present Address: ETH Zürich, Labor für Hochenergiephysik, CH-8093 Zürich, Switzerland.
**Present Address: CERN, Division PPE, CH-1211 Genève 23, Switzerland.

subject of several studies to determine escape and spreading width of the IAS [12].

In this paper we report on investigations of the proton decay of spin-isospin strength, especially of the Gamow-Teller giant resonance in ^{90}Nb, after excitation by the (^{6}Li,^{6}He) reaction using a ^{6}Li beam of 156 MeV. In several studies the (^{6}Li,^{6}He) reaction was found to be a suitable probe for the investigation of spin-isospin modes and for the determination of GT strength with high accuracy [14–18]. Our earlier investigations [15–17] showed over a wide mass range of target nuclei that the GT strength extracted from (^{6}Li,^{6}He) measurements agrees well with results of (p,n) and β-decay measurements. The selection rules $\Delta S=1$ and $\Delta T=1$ of the (^{6}Li,^{6}He) charge exchange reaction are responsible for the high sensitivity towards spin-isospin excitations. The dominating one step character already at beam energies of 25 MeV/nucleon was proven by earlier studies investigating the (^{6}Li,^{6}He) reaction at different bombarding energies [14,19]. In addition the high absorption of the ^{6}Li projectile leads to characteristic angular dependencies for the different multipolarities. Thus $L=0$ monopole strength can be identified by its steep rise to forward angles. Particularly the difference of the spectra taken at $\Theta_{\mathrm{He}}=0°$ and an angle, where the GT strength has already strongly decresed (in our case we used $\Theta_{\mathrm{He}}=2°$), should be dominated by pure $L=0$ strength. From the experimental point of view the charged ^{6}He ejectile allows the use of a magnetic spectrograph. Low background even at zero degree and a high efficiency and energy resolution are advantageous also with respect to coincidence measurements of decay particles.

In the following we describe the experimental techniques of the coincidence experiment in some detail (Sec. II). Section III presents the results of the singles measurements, especially the distribution of GT strength. The results of the decay experiment are described in Sec. IV.

II. EXPERIMENT

The measurements were performed with the momentum analyzed 156 MeV ^{6}Li beam of the Karlsruhe Isochronous Cyclotron. An external electron cyclotron resonance ion source provided a beam of ^{6}Li^{3+} ions with high intensity and stability of $\sim$30 nA, which was an essential presupposition for the feasibility of the experiment [20]. We employed a self-supporting ^{90}Zr target with a thickness of 10 mg/cm^2 and an enrichment of 98%. An overall energy resolution of 420 keV was achieved in the decay measurement limited by the energy loss of the various reaction particles in the target. The ^{6}He ejectiles were measured at extreme forward angles and directly at zero degree using the magnetic spectrograph ''Little John'' [21,22]. At 0° the reaction particles and also the incident beam enter the magnetic spectrograph. Due to its lower magnetic rigidity the beam particles, however, were deflected to the wall of the vacuum chamber, where they were stopped on a movable Faraday cup. The ^{6}He particles were analyzed in the position sensitive focal plane detector, which yielded additional information about time of flight, energy loss and total energy of the detected particles. Thus even at zero degree, we could achieve spectra absolutely free of any experimental background. For the spectroscopy of decay protons a multidetector arrangement of large area

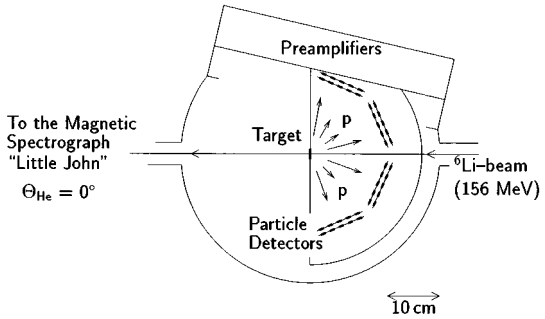

FIG. 1. Schematical drawing of the scattering chamber with the four pairs of the semiconductor strip detectors for coincidence measurements of decay protons.

semiconductor strip detectors was built up within the scattering chamber. The setup with four pairs of detectors covering a total solid angle of 330 msr is shown schematically in Fig. 1. Each detector with an active area of 60 mm$\times$24 mm $=$1440 mm^2 is subdivided into ten independent strips, each 6 mm wide. Thus protons could be measured at 40 different angles simultaneously with an angular resolution better than 1.5°. Two detectors were combined to a counter telescope with a total sensitive thickness of 1000 μm. Thus protons with an energy up to 12 MeV could be stopped completely and the region of excitation energy from the proton threshold at 5 up to 17 MeV could be observed. We restricted the set up of the detectors to backward angles covering a region between 70° and 170° to avoid the detection of protons from quasifree charge exchange process, which is considered as the main background component at forward angles. At zero degrees the whole setup is completely symmetric to the beam direction, at two degrees the deviation from symmetry is small. This leads to a reduction of systematic errors and by averaging the ^{6}He-p angular correlation to a model independent extraction of branching ratios for the transition to the final nucleus ^{89}Zr. This experimental environment with a high flux of light ions and neutrons leads to some radiation damage of the counters. Although clearly observed they did not impair seriously the performance of the experiment and could be partly annealed [23]. With this detector arrangement the measurement of decay protons was possible with rather high energy and angular resolution at a wide range of angles, simultaneously. Specifications about the used detectors and their optimization for the (^{6}Li,^{6}Hep) experiment are given elsewhere [24,25].

III. RESULTS OF THE SINGLES MEASUREMENTS

In a first step we measured and analyzed singles spectra of the (^{6}Li,^{6}He) charge exchange reaction in the angle region between zero and eight degrees. From this for the coincidence measurement reaction angles of 0° and 2° were fixed, where the GT strength is in its maximum and close to its first minimum, respectively. Singles spectra, linearized in energy, of the reaction ^{90}Zr(^{6}Li,^{6}He)^{90}Nb at 0° and 2° are presented in Fig. 2. At zero degrees a significant population of the Gamow-Teller state at 2.3 MeV and the strong excess of the GT giant resonance at about 9 MeV can be observed. At 2° the GT excitations have almost vanished. The state at 1.0 MeV representing strength with higher multipolarities $L>0$

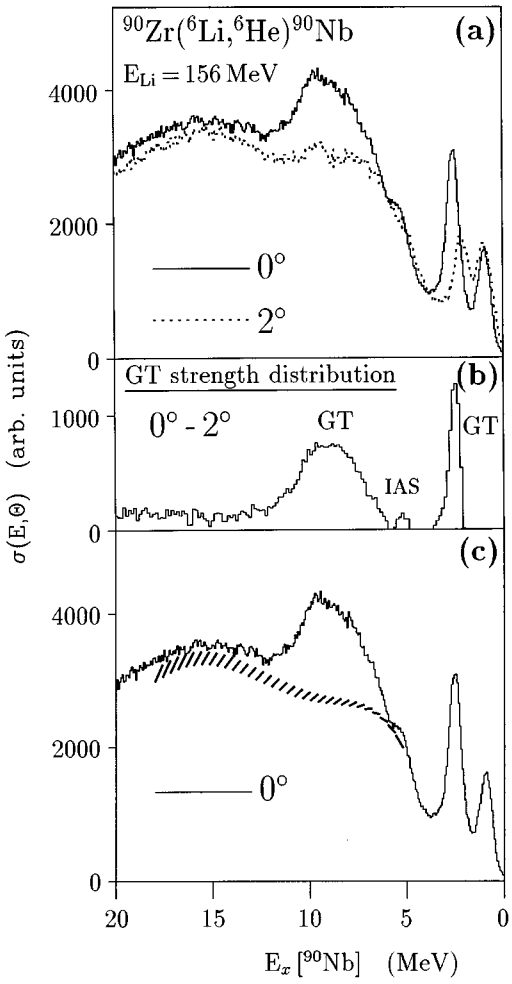

FIG. 2. Spectra of the (^{6}Li,^{6}He) reaction on ^{90}Zr at $\Theta_{He}=0°$ and $\Theta_{He}=2°$ (a) and the difference spectrum (b). 0° spectrum with the physical continuum used for the determination of the giant resonance's cross section (c).

hardly changes in this forward region. At excitation energies around 17 MeV the broad peak corresponds to the well known spin-dipole resonance (SDR) [5] with multipolarity $L=1$. It appears on a broad nonresonant physical continuum from quasifree charge exchange and contributions from higher multipolarities, which almost does not change its shape and strength between zero and two degrees. A small excess at the position of the IAS at 5.1 MeV gives some indication of only a very small excitation of non-spin flip strength with $\Delta S=0$. This confirms the one step character of the (^{6}Li,^{6}He) reaction at the energy of 26 MeV/nucleon and the good suppression of background with $\Delta S=0$. Additionally all spectra even at higher reaction angles slightly decrease towards higher excitation energies indicating that multistep processes do not contribute significantly to the reaction mechanism.

Due to the forward peaked angular distribution of the GT resonances and the flat angular dependencies of higher multipolarities the difference spectrum in Fig. 2(b) gives the distribution of GT strength with little uncertainties from dipole strength and the quasifree continuum, which can change in this forward region. In the difference spectrum the IAS can be detected more clearly, but nevertheless the suppression of non-spin flip transition is still better than in (p,n) measurements at much higher energies. Because $\Delta S=0$ strength is expected to be concentrated in the IAS we can conclude that the difference spectrum presents the distribution of pure GT strength ($\Delta S=\Delta T=1$) with rather high precision. From the difference spectrum the excitation energy and the width of the GT giant resonance was determined to $E_x=8.9\pm0.1$ MeV and $\Gamma=4.1\pm0.1$ MeV. With reduced uncertainties this result is in good agreement with our earlier works [15] and measurements using other probes [3,5]. It seems remarkable that by using this subtraction method GT strength can be identified also in the region above the GT giant resonance bump. The strength can be even reduced by the tentatively increasing spin dipole resonance. Theoretical works have predicted such a flat distribution of GT strength embedded in the continuum as an effect of coupling of the initial $1p$-$1h$ doorway state to $2p$-$2h$ and even more complex configurations [1,28,29]. The difficulties in identifying this structureless strength by performing, e.g., a multipole decomposition [30] was discussed to be one reason for the missing GT strength. From the difference spectrum the B(GT) sum rule value can be easily determined. A Q-value correction is necessary for high lying strength which was performed using a distorted-wave Born approximation (DWBA) calculation as described in Refs. [15,17]. Using the well established B(GT) value for the GT transition to the low lying 2.3 MeV state for normalization [3,4] we extracted a sum rule value of $B(\mathrm{GT})=20.0^{+6.0}_{-3.0}$ or 66^{+20}_{-10}% in units of the Ikeda sum rule up to 20 MeV excitation energy. The GT giant resonance (6 MeV$<E_x<$12 MeV) alone provides 38 ± 5%. In comparison to the results of earlier measurements [15], where the errors due to poor statistics played an important role, in the presented data the statistical error can be neglected. The given systematic errors are mainly estimated from normalization uncertainties. The B(GT) value is in agreement with earlier measurements using refined analyses with special attention to the choice of the background of the nonresonant continuum [6,31]. Following the argumentation of Gaarde *et al.* [6], that 20 to 30% of the whole GT strength is shifted to the region of the delta isobar excitation, this means that almost 90% of the strength accessible in our experiment could be identified without the problem of fixing a more or less arbitrary background [5]. An additional uncertainty may arise from strength with higher multipolarities increasing in the angular region between 0° and 2°. As mentioned above spin dipole strength with $L=1$ can clearly be identified in the excitation spectra at $E_x=17$ MeV. Theoretical calculations predict $L=1$ strength also in the region of the GT giant resonance [28,29]. Dipole excitations, however, show a tentative increase at forward angles leading to the larger positive error of our sum rule values. The exclusive coincidence measurements presented in the next sections will provide additional information to distinguish the contributions of different multipolarities.

For the extraction of the angular distribution of the GT giant resonance the shape of the nonresonant continuum was fixed by subtracting the GT monopole strength after normalization to the content of the peak at 2.3 MeV. The result is indicated by the dashed band in Fig. 2(c) together with the 0° spectrum. The width of the band represents the uncertainties from normalization and higher multipolarities, especially

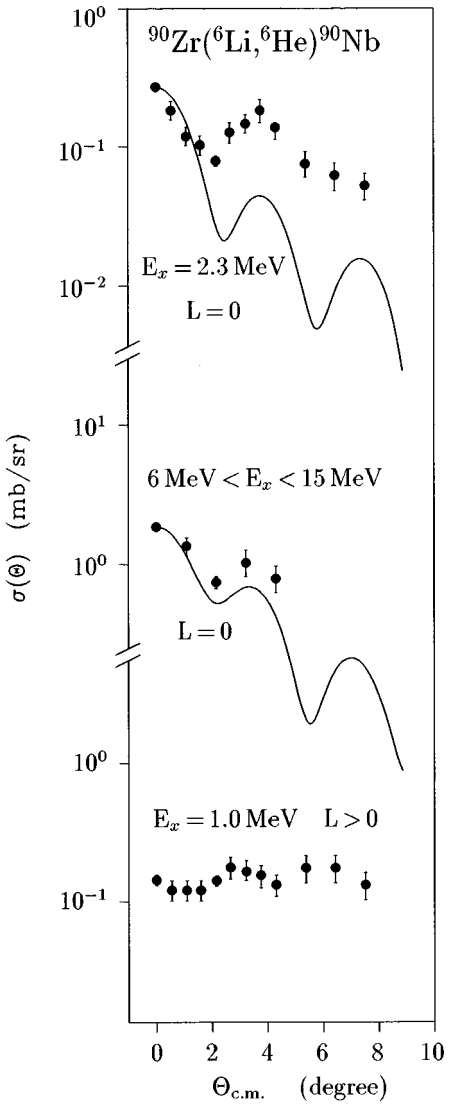

FIG. 3. Experimental angular distributions of the (^{6}Li,^{6}He) reaction on ^{90}Zr together with DWBA calculations.

in the region of the spin dipole resonance. The experimental angular distributions of Fig. 3 were compared to a microscopic DWBA calculation using the computer code DWUCK4 [26]. The form factors were calculated with random-phase approximation (RPA) wave functions and a G matrix of Nakayama including central and tensor terms [27]. At 0° the contribution of the tensor component is small. The curves were adjusted to the data point at zero degree. The monopole character of both GT excitations with a steep increase at forward angles and the flat angular distribution of the higher L state at 1.0 MeV can be clearly observed.

IV. MEASUREMENTS OF THE PROTON DECAY

A. Analysis of the data

A ^{6}He spectrum on condition that a decay proton was detected in coincidence to the ^{6}He is shown in the upper part of Fig. 4. The contribution of accidental coincidences is subtracted. Above the proton threshold at 5.08 MeV the decay via proton emission to the final nucleus ^{89}Zr is energetically allowed, but still strongly supressed up to about 7 MeV excitation energy by the high Coulomb and centrifugal barriers. Therefore the probability for proton decay increases slowly. In the giant resonance region up to the neutron decay threshold at 10.11 MeV proton decay is the only allowed particle decay channel, but also below the neutron threshold a proton yield corresponding to the full excited strength in ^{90}Nb cannot be observed. This is explained by the continuum of quasi-free charge exchange reactions in the free excitation spectrum leading to no proton emission in backward directions. Another reason is the still high probability of γ decay because of the high Coulomb barrier for a proton leaving the nucleus.

For the two marked excitation energy regions A and B, final state spectra were obtained by using additionally the energy information of the proton detectors. For both decay spectra in the lower part of Fig. 4 the two angle settings for the ^{6}He detection were summed up for statistical reasons. The resolution in the decay spectra is sufficient to identify the decay into the first low lying states in ^{89}Zr. Due to the preceding (^{6}Li,^{6}He) charge exchange reaction the decay via protons is leading to neutron hole states in the daughter nucleus. Thus the low lying peaks in the decay spectra can be assigned to well known neutron hole states, e.g., the ground state with spin $J^{\pi}=9/2^{+}$ and the $1/2^{-}$ and $3/2^{-}$ first and second excited state at 0.58 and 1.09 MeV, respectively. The next peak represents a mixture of a few states at about 1.5 MeV among others a state with $J^{\pi}=5/2^{-}$ at 1.45 MeV. At higher excitation energies in ^{89}Zr the final state spectrum for the decay of the GT giant resonance region (A) strongly decreases in spite of a higher density of reachable final states, due to the high Coulomb barrier for the low energetic protons feeding these states. For the higher energy bin (B) above the GT giant resonance much more final states can be reached. It should be dominated by the nuclear continuum and modes with higher multipolarity and only a small component of monopole strength. The decay spectrum is dominated by a broad bump at higher excitation energies, but in addition also a clear population of the low lying neutron hole states mentioned above can be seen.

From the decay spectra relative branching ratios $\Gamma_{\mathrm{rel}p_i}$ can be deduced for the different proton groups. It is defined as the ratio of protons decaying to a definite final state p_i to the number of all detected coincident protons:

$$\Gamma_{\mathrm{rel}p_i}=\Gamma_{p_i}/\sum_i \Gamma_{p_i}. \tag{4.1}$$

For a model independent extraction of the relative branching ratios we profit from the large area proton detectors covering almost the whole region of backward angles, which leads to an averaging over effects of the angular correlations. This method is confirmed by theoretical calculations as well as the measured angular correlations (Secs. IV B and IV C) showing a flat angular dependence. In Fig. 5 the experimental relative branching ratios for the four lowest states in ^{89}Zr are presented for 0.5 MeV energy bins of the excited strength in ^{90}Nb with the ^{6}He measured at zero degrees. Just above the threshold for proton emission the decay to the ground state is the only allowed transition. But as mentioned above, due to the high Coulomb and angular momentum barrier a decay to the low lying states is strongly suppressed and

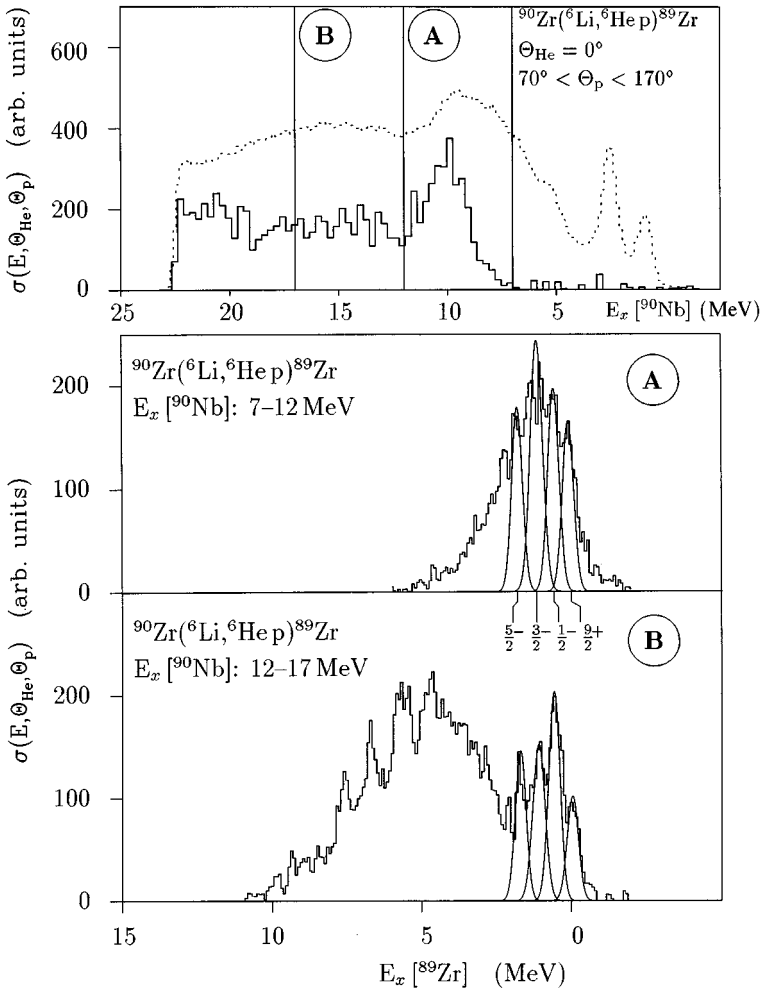

FIG. 4. ^{90}Zr(^{6}Li,^{6}He)^{90}Nb in coincidence with a decay proton (upper part). The 0° singles spectrum is indicated. Final state spectra for a decay to the residual nucleus ^{89}Zr for the two energy bins marked above (lower parts).

could not be evaluated with satisfying accuracy up to excitation energies of about 7 MeV. Starting from this value the decay to the ground state is the most favored transition. But with higher energies it strongly decreases and the decay to excited states becomes more probable. The general slope of the relative branching ratios with a smooth increase above the threshold for the respective proton groups and the following slowly decrease reflects the influence of the Coulomb barrier for proton emission leading to broad curves without significant steps or structures. The theoretical relative branching ratios shown in Fig. 6 were calculated in the framework of a pure statistical decay. Assuming that the initial particle hole configuration of the GT giant resonance is completely thermalized they only depend on the transmission coefficients of the decay particles, which can be calculated from the energy difference and the spins of the decaying mode and of the final states. The transmission coefficients were calculated using the standard optical potential of Ref. [33]. The relative branching ratios for the four lowest states in ^{89}Zr, plotted in Fig. 6, were calculated for modes in ^{90}Nb with different spins. All final states up to an excitation energy of 2 MeV in ^{89}Zr were taken into account. For the giant resonance region in ^{90}Nb a decay into higher lying states in ^{89}Zr is strongly suppressed due to the Coulomb barrier. At higher excitation energies a decay into states above 2 MeV in ^{89}Zr becomes possible and the theoretical relative branching ratios should overestimate the measured data points. For the relatively low energetic protons under consideration the centrifugal barrier inhibits the proton decay with a high transfer of angular momentum. Thus strength with high spin dominantly decays to states with high spin and modes with low spin prefer low spin final states. Therefore the population of the neutron hole states in ^{89}Zr with such different spins as $9/2^+$ of the ground state and $1/2^-$ of the first excited state is strongly dependent on the spin of the decaying strength. This ''spin-filter'' effect was also already applied to the neutron decay of isoscalar electric giant resonances [34] and can be used to determine the relative contribution of modes with different spins and multipolarities to the excited strength.

B. Decay of the Gamow-Teller giant resonance

As in the singles spectra it is the comparison between 0° and 2° measurements from which we can get more information on the GT giant resonance. The maximum minimum method is applied to the decay spectra in Fig. 7. In Figs. 7(a) and 7(b) the final state spectra for a proton decay to ^{89}Zr measured at a spectrometer setting of 0° and 2° are compared, in Fig. 7(c) the difference of both spectra presents

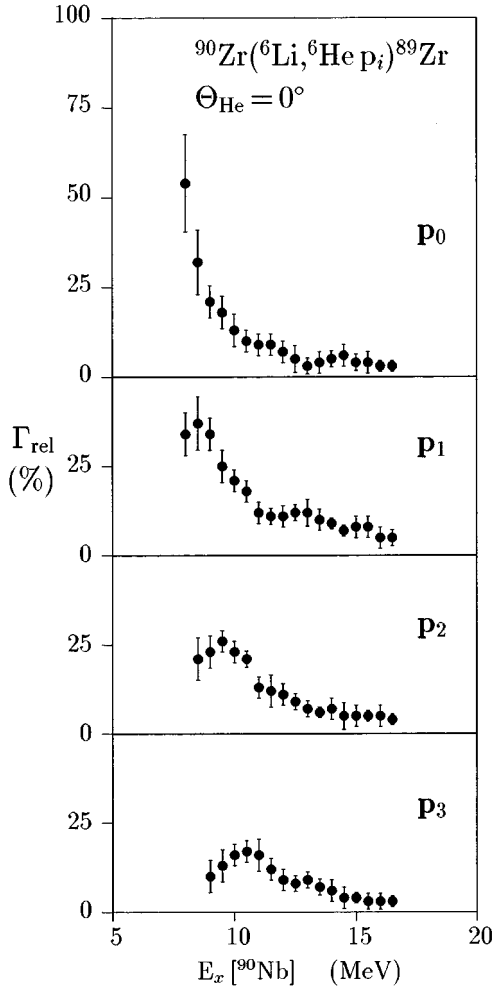

FIG. 5. Experimental relative branching ratios for a decay of strength in ^{90}Nb by the (^{6}Li,^{6}He) reaction at 0° to the four lowest states in ^{89}Zr as a function of the excitation energy in ^{90}Nb.

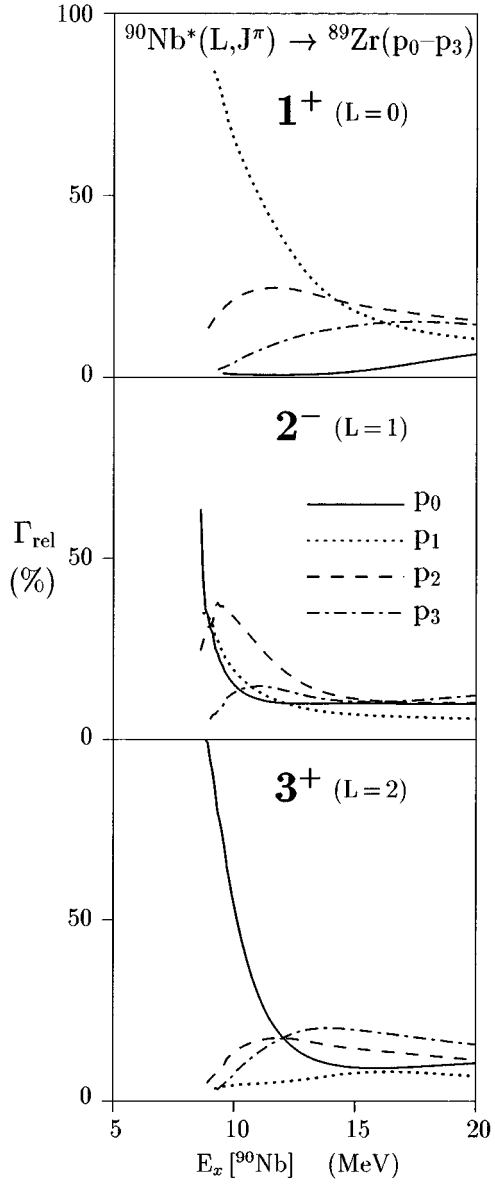

FIG. 6. Theoretical branching ratios for a decay of different spin-isospin modes in ^{90}Nb to the four lowest states in ^{89}Zr calculated in the statistical model.

almost exclusively the decay of the GT giant resonance. The decay spectra were generated under the restriction of the excitation energy in ^{90}Nb to the giant resonance region between 8.0 and 12.0 MeV. Thus it is shifted to the higher energy side of the giant resonance avoiding strong threshold effects just above 5.1 MeV but it is covering the main region of proton decay. As in Fig. 4 a clear population of low lying neutron hole states can be observed indicated by Gaussian curves adjusted to the data. In the fit the experimental resolution of 420 keV was held fixed. The intensity, however, of the various states is strongly different for the two measured angles, where GT strength is in a maximum and in a minimum. Comparing the two decay spectra and regarding the difference spectrum it is obvious that the GT giant resonance is decaying preferably to states with low spins such as the $1/2^-$ first excited and the $3/2^-$ second excited state. In contrast no decay to the ground state with its high spin of $9/2^+$ can be observed. This state is slightly more populated at 2° that an 0°, which can be explained by underlying strength with higher multipolarities especially dipole strength that shows a tentative rise from 0° to 2° and has a rather high probability for a decay to the $9/2^+$ ground state of ^{89}Zr as shown in Fig. 6.

More quantitatively the decay to the three lowest states is evaluated in Table I, where the percentual contributions $\Gamma_{p_i}/\Sigma_{i=0}^{2}\Gamma_{p_i}$ of the three lowest states are listed. The other levels were omitted because only the three lowest states can be identified clearly in the decay spectra. The proton group p_3 is already a mixture of several states with different spins making the interpretation more difficult. In spite of the large uncertainties we can conclude that with respect to transitions to the three lowest states in ^{89}Zr the decay to the first excited state has a probability of about 70% and to the second excited state of around 30%, while no decay to the ground state can be observed. In view of the RPA wave functions for the GT giant resonance [27], which were also used to calculate the angular distributions of Fig. 3, the main proton particle neutron hole components of the GT giant resonance are the $1g_{9/2}^{n-}1g_{7/2}^{p}$ spin flip and $1g_{9/2}^{n-}1g_{9/2}^{p}$ core polarization states which would lead to a significant population of the $J^{\pi}=9/2^+$

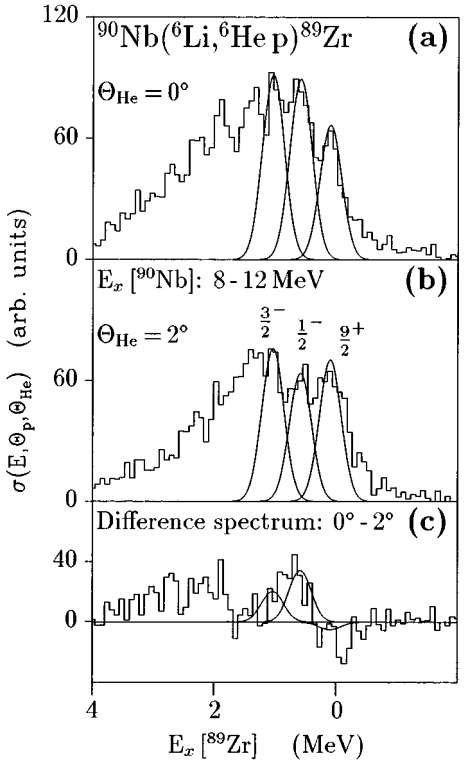

FIG. 7. Decay spectra of protons from the GT resonance region in ^{90}Nb to ^{89}Zr at $\Theta_{He}=0°$ (a) and $\Theta_{He}=2°$ (b). Difference spectrum (c).

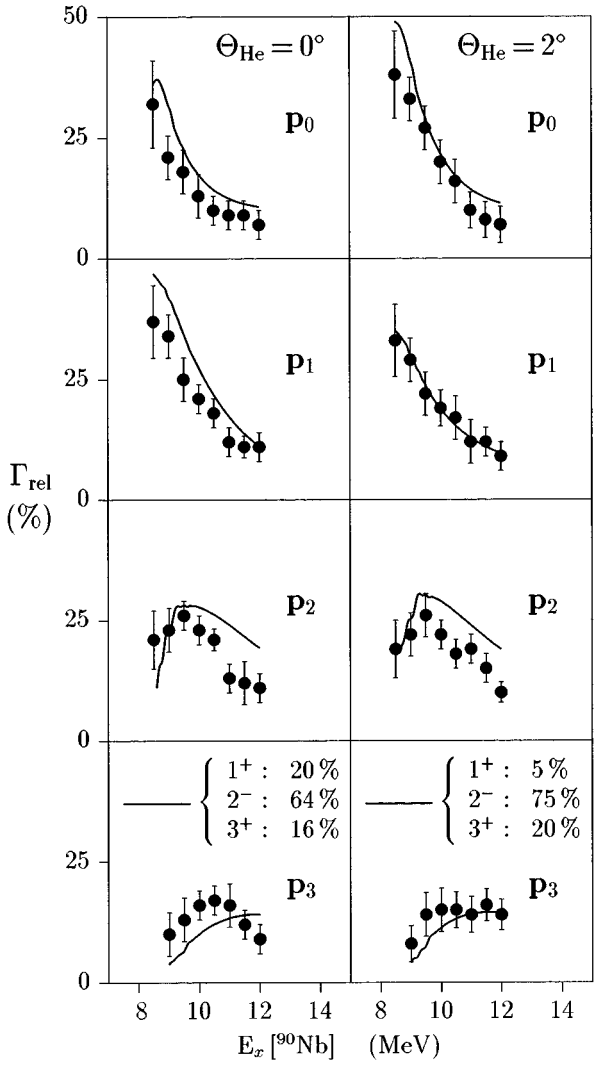

FIG. 8. Relative branching ratios for a decay to the four lowest states in ^{89}Zr from the GT giant resonance region together with calculations in the statistical model.

ground state in ^{89}Zr in the case of a direct decay. Although the transmission coefficients are very small, more than 60% of a possible proton decay should lead to the ground state in ^{89}Zr. The low spin states with high transmission coefficients should be much less populated. The opposite result can be found in the model of a statistical decay. Here the transmission coefficients alone determine the decay characteristics, after the initial particle-hole structure of the GT giant resonance has been spread out to many more complicated states. The high transmission coefficients of transitions to the low spin states are favoring the decay to the first and second excited states, while the ground state is almost not populated. From these results collected in Table I we can conclude that although the experimental uncertainties are relatively high an unambiguous signature for a predominant statistical decay of the GT giant resonance is present. However, it should be mentioned that a small direct decay component cannot be ruled out. A small branching to the ground state leading immediately to a nonstatistical decay mechanism is still possible and may be canceled by the decay of strength with high L feeding the ground state in ^{89}Zr and increasing between

TABLE I. Experimental relative contributions in percent for a decay of the GT giant resonance to the three lowest states in ^{89}Zr and the theoretical predictions for either direct or statistical decay.

	p_0 $9/2^+$	p_1 $1/2^-$	p_2 $3/2^-$
Experiment	0±12	70±10	30±12
Direct decay	65	30	5
Statistical decay	1	73	26

0° and 2°. A comparable decay experiment studying the decay of the GT giant resonance in ^{208}Bi excited by the reaction ^{208}Pb(^{3}He,t) found a dominant statistical decay, too, but also a small direct component of proton decay of (4.9±1.3) % [13].

Presuming a pure statistical decay it should be possible to determine the composition of different spin modes in the decaying nucleus by comparing the relative branching ratios of Fig. 5 with calculations in the statistical model. This was done in the energy region 8.0 MeV$\leqslant E_x \leqslant$12.0 MeV separately for 0° and 2° with results shown in Fig. 8. As possible excitations besides the GT monopole mode spin dipole with $J^\pi=2^-$ and spin quadrupole strength ($J^\pi=3^+$) were taken into account as proposed by theoretical works [28,29]. For the GT strength a Gaussian shape with the resonance parameters taken from Sec. III was assumed while for the higher L modes an uniform relative strength distribution in the observed region of excitation energy was assumed. A best description of the decaying strength was achieved with 20% GT strength and 64% spin dipole and 16% spin quadrupole strength at zero degrees and with 5% GT strength and 75% spin dipole and 20% spin quadrupole strength at two de-

grees. The results of the calculations are presented in Fig. 8 as solid lines together with the experimental data. If a direct decay component is present, the ground state with the high spin of $9/2^+$ will also be fed by the GT giant resonance and the deduced strength contribution of higher multipolarities would be reduced. Transformed into absolute units of cross sections the above strength decomposition confirms the evaluation of the singles measurements: The steep decrease of the GT strength between 0° and 2° was already seen in the singles spectra of Fig. 2. The values of the angular distributions of Fig. 3 are confirmed. By the high decay probability to the $9/2^+$ ground state strength with higher multipolarities $L \geqslant 1$ is clearly identified embedded in the continuum below the GT giant resonance. If a direct decay component is present, which is probable from other experiments, the high spin ground state is also fed by the GT giant resonance and the deduced strength contribution of higher multipolarities would be reduced. Spin dipole strength, however, is slightly increasing between 0° and 2°. In Sec. III it was already discussed that the presence of spin dipole strength leads tentatively to an underestimation of GT strength applying the maximum-minimum method to the 0° and 2° spectra of Fig. 2. The sum rule value extracted from the difference spectrum may be a little too small. On the other hand the knowledge of the different decay behaviors of GT strength and modes with higher transfer of angular momentum can be used to identify GT strength independently. Assuming a statistical decay, the transition to the ground state in ^{89}Zr is a clear signature of the decay of non-GT strength as can be seen from the results above and from the theoretical relative branching ratios of Fig. 6, where for GT strength ($J^\pi = 1^+$) only a neglectable probability for a decay to the proton group p_0 was observed. Therefore, the transition strength to the ground state can be used as a built-in normalization for strength with higher L. This is presented in Fig. 9 where the coincident ^{6}He spectra are plotted under the restriction of a decay to the various proton groups p_0 to p_3. For a proton emission to the ^{89}Zr ground state the 2° spectrum lies above the 0° spectrum showing the slightly increasing strength of higher multipolarities (especially $L=1$). In contrast the ^{6}He spectra measured at 0° exceed the 2° spectra for a proton decay to the excited states with lower spins, describing the decay of the GT strength. If we normalize the 0° and 2° spectra according to the strength in Fig. 9(a), as is done globally in Figs. 9(e) and 9(f), we find a clear excess of the 0° measurement towards the 2° measurement for a decay to $p_1 - p_3$ showing that GT strength is not only identified in the immediate GT giant resonance region but also as a small but significant flat distribution at higher excitation energies. The poor statistics do not allow us to evaluate this result in a more quantitative way, but nevertheless by use of this decay normalization method GT strength was again identified also at higher excitation energies.

The He-p angular correlation for a decay of the GT giant resonance region to the four lowest states in ^{89}Zr are presented in Fig. 10, again separately for 0° and 2° measurements. The decay angle is given in center-of-mass coordinates of the decaying intermediate nucleus ^{90}Nb. The error bars in the y directions are due to the statistical uncertainties alone while the errors in the x directions represent the finite solid angle of the detector segments under consideration. In

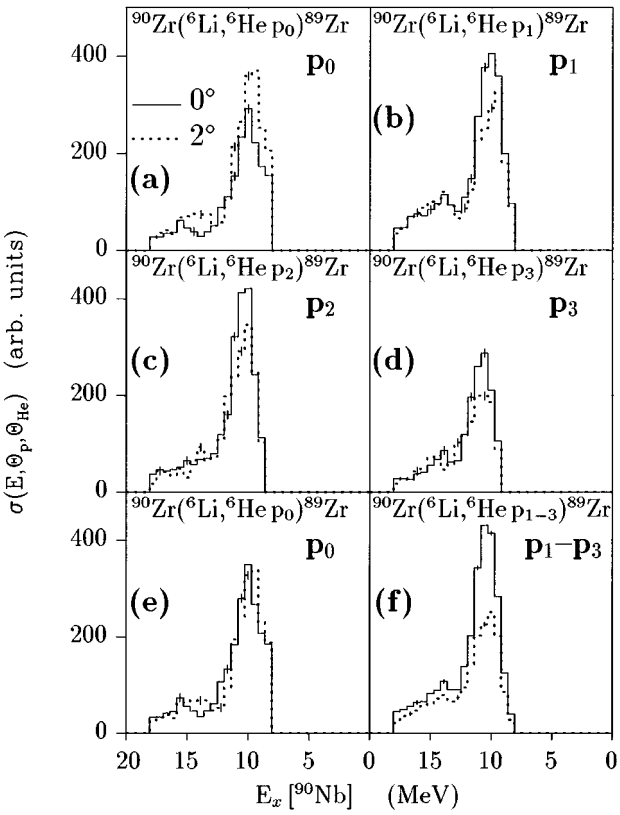

FIG. 9. Excitation spectra of ^{90}Nb coincident to proton decays to the four low lying states in ^{89}Zr at $\Theta_{He}=0°$ (solid line) and $\Theta_{He}=2°$ (dotted line) (a)–(d). Spectra (e) and (f) show the coincident excitation spectra for a decay to the proton group p_0 and p_1-p_3, where the 0° and 2° spectra are normalized in accordance to the strength decaying to p_0.

principle additional information on the multipolarity of the excited strength should be obtained from the angular behavior of the correlation function [32]. But due to the complex spin couplings for a proton decay, only flat angular correlation functions are predicted also for a decay of modes with higher multipolarity by partial waves with high angular momentum. Legendre polynomials of maximum order $k_{max}=2$ were adjusted to the data represented by the solid lines in Fig. 10. The corresponding coefficients are listed in Table II. As expected the angular correlation are relatively flat, only the decay to the first excited state p_1, shows an increase to 180° indicating again the presence of strength with higher multipolarity.

C. Decay of the strength above the giant resonance region

The high lying strength between 12 and 17 MeV excitation energy is located above the GT giant resonance and already above the threshold for neutron decay thus reducing the proton decay branch. As it is dominated by the nuclear continuum and modes with higher multipolarities that do not change significantly in the forward angle region, the measurements of 0° and 2° were summed up to achieve better statistics. In Fig. 11(a) the proton decay spectrum for the energy region between 12 to 17 MeV in ^{90}Nb from Fig. 4 is displayed again. The decay of this energy region leads mainly to a broad bump of emitted protons in the high lying

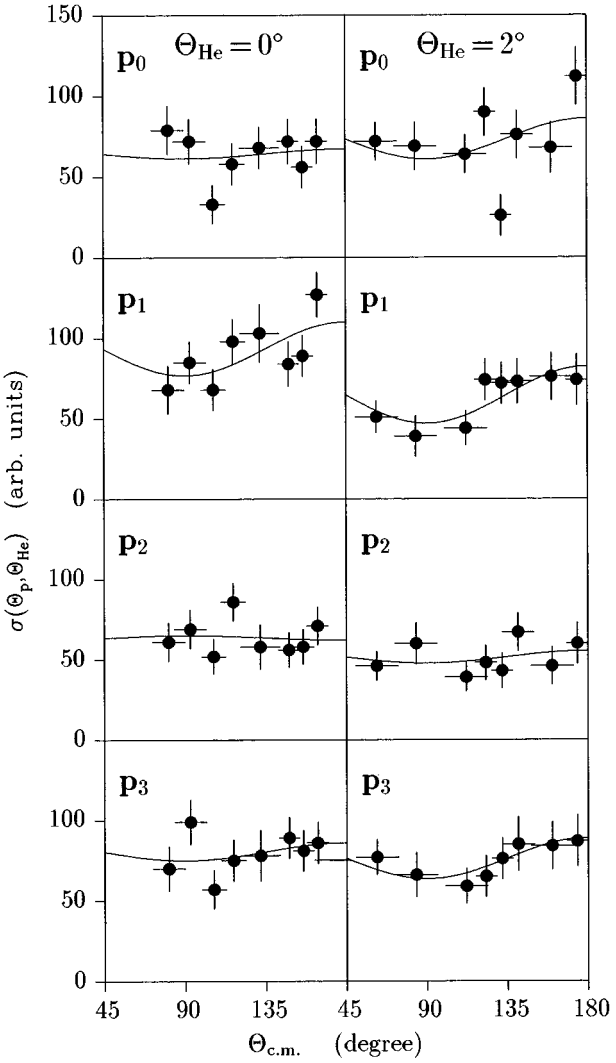

FIG. 10. ^{6}He-p angular correlations for a decay of the GT giant resonance region to the four lowest states in ^{89}Zr. The solid lines represent fits of Legendre polynomials.

region of high level densities in ^{89}Zr. This distribution of low energetic protons is well described by a calculation in the statistical decay model represented by the solid line. The evaporationlike shape of the proton spectrum according to the formula $N(E_p)=E_p\exp(-E_p/T)$ must be modified by a Gamow factor describing the hindrance of penetration for very low energetic protons. The angular correlation measured for the protons decaying to the broad distribution is plotted in Fig. 11(c). It is found to be nearly isotropic again in agreement with a statistical decay mechanism of a superposition of many multipolarities.

TABLE II. Legendre parameters for the angular correlations of Fig. 10.

		p_0 $9/2^+$	p_1 $1/2^-$	p_2 $3/2^-$	p_3 $5/2^-$
0°	A_0	61.4±4.8	87.2±5.0	63.7±4.3	77.7±4.8
	a_2	0.10±0.14	0.24±0.11	−0.03±0.12	0.11±0.11
2°	A_0	67.6±5.1	58.2±4.5	48.5±4.0	71.7±4.8
	a_2	0.18±0.16	0.45±0.18	0.14±0.18	0.24±0.15

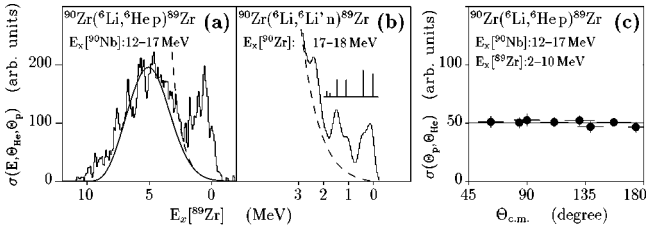

FIG. 11. Final state spectrum from the proton decay of the energy region in ^{90}Nb above the GT giant resonance (a). For comparison spectrum (b) shows the decay spectrum of the neutron decay of the isoscalar giant resonance in ^{90}Zr to the same final states in ^{89}Zr. ^{6}He-p angular correlation for a decay to the broad bump of many levels in ^{89}Zr (c).

On the other hand, a clear population of the low lying neutron hole states by high energetic decay protons can be observed. These transitions cannot be reproduced by a statistical calculation alone. They represent a direct decay component of resonant strength. The spin dipole resonance (SDR) is visible in the singles spectra (Fig. 2) as a broad bump around 17 MeV, but also other modes with higher L should be present comparable to the region of the GT giant resonance. It can be informative to compare this result with a neutron decay spectrum of the $E0$ isoscalar electric giant resonance in ^{90}Zr after excitation by inelastic ^{6}Li scattering leading to the same neutron hole states in ^{89}Zr [Fig. 11(b)] [35]. Again the exponential distribution of statistical decay neutrons with low energies can be observed, of course without the influence of the Coulomb barrier, and again the population of the low lying neutron hole states is obvious. In both cases the results can be interpreted in terms of a dominant statistical decay with a small but significant direct decay component that seems to be a common feature of collective nuclear excitations in medium and heavy nuclei.

V. SUMMARY

The excitation and decay of collective spin-isospin excitations in ^{90}Nb has been measured using the (^{6}Li,^{6}He) reaction on a ^{90}Zr target by use of the magnetic spectrograph ''Little John'' and a semiconductor multidetector array.

The investigations of the decay characteristics of the Gamow-Teller giant resonance showed a dominant statistical damping. For the Gamow-Teller giant resonance a direct decay component is not observed but cannot be excluded. Even at higher excitation energies strong evidence for a direct decay component was found. The measured relative branching ratios for a proton decay to the four low lying neutron-hole states in ^{89}Zr were compared to calculations in the statistical model. A rather good agreement could be achieved if additional strength with higher multipolarities $L\geqslant 1$ is taken into account. Spin dipole strength also visible as a broad resonance at around 17 MeV excitation energy in the singles spectrum can be clearly identified in the continuum under the GT giant resonance. An investigation of the proton and competing neutron decay extended to higher excitation energies in ^{90}Nb could give more information about the damping mechanism and the composition of nuclear continuum and resonant strength.

The distribution of Gamow-Teller strength was evaluated in detail. The excitation energy and total width of the

Gamow-Teller giant resonance was extracted from the subtraction spectrum of the 0° and 2° measurement. The sum rule value for the energy region up to 20 MeV was determined to be 66^{+20}_{-10}% of the Ikeda sum rule. Remarkable Gamow-Teller strength above the giant resonance was detected and confirmed by the characteristic decay behavior.

ACKNOWLEDGMENTS

We wish to thank the staff of the Karlsruhe Cyclotron Laboratory for their cooperation. This work was funded by the German Federal Minister for Education and Research (BMBF) under Contract No. 06ER262I and by the Forschungszentrum Karlsruhe.

[1] F. Osterfeld, Rev. Mod. Phys. **64**, 491 (1992).
[2] K. Ikeda, Prog. Theor. Phys. **31**, 434 (1964).
[3] D. E. Bainum, J. Rapaport, C. D. Goodman, D. J. Horen, C. C. Foster, M. B. Greenfield, and C. A. Goulding, Phys. Rev. Lett. **44**, 1751 (1980).
[4] C. D. Goodman, C. A. Goulding, M. B. Greenfield, J. Rapaport, D. E. Bainum, C. C. Foster, W. G. Love, and F. Petrovich, Phys. Rev. Lett. **44**, 1755 (1980).
[5] C. Gaarde, J. Rapaport, T. N. Taddeucci, C. D. Goodman, C. C. Foster, D. E. Bainum, C. A. Goulding, M. B. Greenfield, D. J. Horen, and E. Sugarbaker, Nucl. Phys. **A369**, 258 (1981).
[6] C. Gaarde, Nucl. Phys. **A396**, 127c (1983).
[7] T. N. Taddeucci, C. A. Goulding, T. A. Carey, R. C. Byrd, C. D. Goodman, C. Gaarde, J. Larsen, D. J. Horen, J. Rapaport, and E. Sugarbaker, Nucl. Phys. **A469**, 125 (1987).
[8] J. Jänecke, K. Pham, D. A. Roberts, D. Stewart, M. N. Harakeh, G. P. A. Berg, C. C. Foster, J. E. Lisantti, R. Swafta, E. J. Stephenson, A. M. van den Berg, S. Y. van der Werf, S. E. Muraviev, and M. H. Urin, Phys. Rev. C **48**, 2828 (1993).
[9] K. T. Knöpfle and G. J. Wagner, in *Electric and Magnetic Giant Resonances in Nuclei, Vol. 7 of International Review of Nuclear Physics*, edited by J. Speth (World Scientific, Singapore, 1991), p. 234.
[10] W. Eyrich, K. Fuchs, A. Hofmann, U. Scheib, H. Steuer, and H. Rebel, Phys. Rev. C **29**, 418 (1984).
[11] C. Gaarde, J. S. Larsen, A. G. Drentje, M. N. Harakeh, and S. Y. van der Werf, Phys. Rev. Lett. **46**, 902 (1981).
[12] S. Y. van der Werf, M. N. Harakeh, and E. N. M. Quint, Phys. Lett. B **216**, 15 (1989), and references therein.
[13] H. Akimune, I. Daito, Y. Fujita, M. Fujiwara, M. B. Greenfield, M. N. Harakeh, T. Inomata, J. Jänecke, K. Katori, S. Nakayama, H. Sakai, Y. Sakemi, M. Tanaka, and M. Yosoi, Phys. Rev. Lett. **323**, 107 (1994); Phys. Rev. C **52**, 604 (1995); Y. Fujita, H. Akimune, I. Daito, M. Fujiwara, M. N. Harakeh, T. Inomata, J. Jänecke, K. Katori, H. Nakada, S. Nakayama, A. Tamii, M. Tanaka, H. Toyokawa, and M. Yosoi, Phys. Lett. B **365**, 29 (1996); M. Fujiwara, H. Akimune, I. Daito, H. Ejiri, Y. Fujita, M. B. Greenfield, M. N. Harakeh, T. Inomata, J. Jänecke, S. Nakayama, N. Takemura, A. Tamii, M. Tanaka, H. Toyokawa, and M. Yosoi, Nucl. Phys. **A599**, 223c (1996).
[14] J. S. Winfield, N. Anantaraman, S. M. Austin, Z. Chen, A. Galonsky, J. van der Plicht, H. L. Wu, C. C. Chang, and G. Ciangaru, Phys. Rev. C **35**, 1734 (1987).
[15] H. Wirth, E. Aschenauer, W. Eyrich, A. Lehmann, M. Moosburger, H. Schlösser, H. J. Gils, H. Rebel, and S. Zagromski, Phys. Rev. C **41**, 2698 (1990); H. Wirth, Ph.D. thesis, Erlangen, 1990.
[16] M. Moosburger, E. Aschenauer, H. Dennert, W. Eyrich, A. Lehmann, R. Rudeloff, H. Schlösser, H. Wirth, H. J. Gils, H. Rebel, and S. Zagromski, Phys. Rev. C **41**, 2925 (1990).
[17] E. Aschenauer, H. Dennert, W. Eyrich, A. Lehmann, M. Moosburger, H. Schlösser, H. Wirth, H. J. Gils, H. Rebel, and S. Zagromski, Phys. Rev. C **44**, 2771 (1991).
[18] H. Laurent, S. Gales, D. Beaumel, G. M. Crawley, J. E. Finck, S. Fortier, J. M. Maison, C. P. Massolo, D. J. Mercer, J. S. Winfield, and G. H. Yoo, Nucl. Phys. **A569**, 297c (1994).
[19] N. Anantaraman, J. S. Winfield, S. M. Austin, Z. Chen, A. Galonsky, J. van der Plicht, C. C. Chang, G. Ciangaru, and S. Gales, Phys. Rev. Lett. **57**, 2375 (1986).
[20] R. Ernst, L. Friedrich, E. Huttel, and F. Schulz, Nucl. Instrum. Methods Phys. Res. A **287**, 337 (1990).
[21] H. J. Gils, J. Buschmann, S. Zagromski, J. Krisch, and H. Rebel, Nucl. Instrum. Methods Phys. Res. A **276**, 151 (1989).
[22] H. J. Gils, H. Jelitto, H. Schlösser, S. Zagromski, J. Buschmann, W. Eyrich, A. Hofmann, J. Kiener, A. Lehmann, and H. Rebel, Nucl. Instrum. Methods Phys. Res. A **276**, 169 (1989).
[23] J. Hauffe, W. Eyrich, M. Kirsch, M. Moosburger, and F. Stinzing, Nucl. Instrum. Methods Phys. Res. A **366**, 79 (1995).
[24] N. Scholz, H. Dennert, W. Eyrich, A. Lehmann, M. Moosburger, and H. Wirth, Nucl. Instrum. Methods Phys. Res. A **313**, 233 (1992).
[25] N. Scholz, E. Aschenauer, H. Dennert, W. Eyrich, A. Lehmann, M. Moosburger, H. Wirth, H. J. Gils, H. Rebel, and S. Zagromski, Z. Phys. A **344**, 269 (1993).
[26] P. D. Kunz, computer code DWUCK4 (unpublished); P. D. Kunz (private communication).
[27] W. Unkelbach and K. Nakayama (private communication).
[28] S. Drożdż, V. Klemmt, J. Speth, and J. Wambach, Phys. Lett. B **166**, 18 (1986).
[29] S. Drożdż, F. Osterfeld, J. Speth, and J. Wambach, Phys. Lett. B **189**, 271 (1987).
[30] T. Wakasa, H. Sakai, H. Okamura, H. Otsu, S. Ishida, N. Sakamoto, T. Uesaka, Y. Satou, M. B. Greenfield, N. Koori, A. Okihana, and K. Hatanaka, Phys. Rev. C **51**, R2871 (1995).
[31] F. Osterfeld, Phys. Rev. C **26**, 762 (1982).
[32] S. Devons and L. J. B. Goldfarb, in *Nuclear Reactions III, Handbuch der Physik*, edited by S. Flügge (Springer, Berlin, 1957).
[33] F. G. Perey, Phys. Rev. **131**, 745 (1963).
[34] K. Fuchs, W. Eyrich, A. Hofmann, B. Mühldorfer, U. Scheib, H. Schlösser, and H. Rebel, Phys. Rev. C **32**, 418 (1985).
[35] W. Eyrich, A. Hofmann, A. Lehmann, B. Mühldorfer, H. Schlösser, H. Wirth, H. J. Gils, H. Rebel, and S. Zagromski, *First Topical Meeting on Giant Resonance Excitation in Heavy Ion Collisions*, Legnaro (Padova), Italy, 1987 (unpublished); B. Mühldorfer, Ph.D. thesis, Erlangen, 1986.